



# Spatial multi-games under myopic update rule

Yuanxin Ye<sup>1,2</sup>, Yiran Xie<sup>1,2</sup>, and Bo Yang<sup>1,2,a</sup>

<sup>1</sup> Data Science Research Center, Kunming University of Science and Technology, Kunming 650500, China

<sup>2</sup> Faculty of Science, Kunming University of Science and Technology, Kunming 650500, China

Received 28 December 2021 / Accepted 23 February 2022 / Published online 14 March 2022

© The Author(s), under exclusive licence to EDP Sciences, SIF and Springer-Verlag GmbH Germany, part of Springer Nature 2022

**Abstract.** Considering the population diversity and the limitation of individual information in repeated  $N$ -person games, we study a spatial multi-games model under the myopic rule in this paper, in which two distinct types of players participate in snowdrift game (SG) and prisoner's dilemma game (PDG), respectively. Monte Carlo simulation method is used to study: the effects of game intensity parameters  $b$  and  $\delta$ , noise parameter  $k$  and mixing ratio  $p$  on the frequency of cooperators; the difference between learning update rule and myopic update rule. The results demonstrate that: (1) when the values of  $b$  and  $\delta$  are small, noise parameter  $k$  can promote the emergence of cooperation in SG with myopic update rule; (2) different from learning mechanism, the effect of the parameters  $p$  on the frequency of cooperators is nonmonotonic under myopic mechanism; (3) cooperators can form clusters to resist the invasion of defectors under learning update rule, while cooperators and defectors tend to form the chessboard-like patterns to increase individual payoff under myopic update rule.

## 1 Introduction

In prisoner's dilemma game (PDG) and snowdrift game (SG), selfish individuals pursue the maximization of their own interests, which causes social dilemmas. However, cooperation widely exists in various life systems. Therefore, the research on emergence and maintenance of cooperation among selfish individuals has become an absorbing research problem. Spatial evolutionary game theory is one of the effective ways to research such subjects [1–3]. The players are located on the site of spatial networks (such as two-dimensional regular lattices, small-world networks, and scale-free networks) and play some kind of game (such as PDG and SG) with their neighbors. Then, these individuals update their current strategies by a specific evolutionary rule (such as learning mechanism, myopic mechanism, and aspiration mechanism). After repeated games for many times, the systems will reach a steady state.

Nowak and May [1] first studied the spatial PDG in which players change their strategies by a deterministic evolutionary rule on two-dimensional square lattice. The results indicate that cooperators can form compact clusters to resist the invasion of defectors. That means spatial structure promotes the emergence of cooperation in PDG. Later, Hauert et al. [4] studied the spatial SG in which players change their strategies by a replicator dynamics rule on the regular networks. The results show that cooperators can form many small and isolated patches. That means spatial structure inhibits

the emergence of cooperation in SG. Then, researchers studied the spatial PDG with a learning rule on the random regular graph and the regular small-world network, respectively [5, 6]. The results indicate that the overall fraction of cooperators that survives evolution is sizably enhanced via heterogeneity effects. Later, Santos et al. [7, 8] studied, respectively, the spatial PDG and SG on scale-free networks. The results show that the mechanisms of growth and preferential attachment in networks provide sufficient conditions for cooperation to dominate. Recently, Wang et al. [9] reviewed the fascinating and counterintuitive results of evolutionary games on multilayer networks due to different ways of coupling on network layers, such as the utilities of players, the flow of information and the popularity of different strategies. In addition, the introduction of preference [10, 11], punishment [12–15], reputation [16, 17], memory [18, 19] social diversity [20], coevolutionary mechanism [21], defensive alliance [22] and other factors can also have an effect on the emergence and maintenance of cooperation. The evolutionary rules are another important field in spatial evolutionary game. The general strategy updating rules include: learning rule [2, 4–8] imitating neighbor strategies by a certain probability; aspiration rule [23–27] setting their own desired payoffs; myopic rule [28–31], also known as self-questioning rule [32–38], reflecting on the payoff difference between their positive and negative strategies.

Multi-games model usually involves several payoff matrices and has different forms. Hashimoto [39, 40] first introduced a multi-games model based on the biological and social systems, in which participants play

<sup>a</sup> e-mail: yangbo@kust.edu.cn (corresponding author)

several games simultaneously and obtain benefit from the summation of the rewards of each game. Then, Szolnoki et al. [41] proposed a coevolutionary success-driven multi-games model, in which players revise their payoff matrix by comparing their payoffs from the previous round with the predesigned payoff threshold. Following these researches, Wang et al. [42] studied an evolutionary multi-games model motivated by the fact that the same social dilemma can be perceived differently by different players. In their model, populations are divided into three categories (taking part in the weak PDG, the traditional PDG and SG, respectively) via the value of the sucker's payoff and use different payoff matrices to play with others. The results show that the higher the heterogeneity of the population, the more the evolution of cooperation is promoted. Next, Qin et al. [43] studied the effects of social diversity (rescale the payoffs by the uniform, exponential or power-law distribution) on the promotion of cooperation in spatial multi-games. Later, Li et al. [44] proposed a coevolution mechanism of strategy and game type evolving simultaneously in multi-games model. The results show that this mechanism can effectively solve the collective cooperation problem. Recently, Li et al. found that the mechanism of alliance (forming alliances with the neighbors using the same strategy) [45] and reputation preference (cooperation can increase reputation, and defection can reduce reputation) [46] can promote the emergence of cooperation in the spatial multi-games model. Meanwhile, Liu et al. [47] confirmed that the diversity of interaction intensity (different opponents have different weights) also can enhance the cooperation in spatial multi-games.

Among the previous studies mentioned above, the individual heterogeneity has well been considered in the multi-games model. However, the incomplete information brought by heterogeneity cannot be ignored. It is hard to obtain neighbors' game types and payoffs in the process of game. Based on it, we investigate the spatial multi-games under myopic update rule in this paper. Specifically, the players obtain the actual total payoff by playing with their nearest neighbors adopting present strategy, and obtain the virtual total payoff by playing with their neighbors using anti-strategy. After comparing the actual total payoff with the virtual total payoff, they revise their strategies used in the next round by a certain probability [32–38].

This paper is organized as follows. In Sect. 2, we introduce spatial multi-games model, myopic update rule and Monte Carlo simulation method. In Sect. 3, we analyze and discuss the simulation results. In Sect. 4, we draw some conclusions.

## 2 Spatial multi-games model under myopic update rule

### 2.1 Spatial multi-games model

Players are placed in a two-dimensional  $L \times L$  square lattice with periodic boundary conditions. They only play games with their four nearest neighbors and obtain

benefits. At the beginning, participants are randomly divided into two categories according to the mixing parameter  $p$ . That means the fraction  $p$  of the total players takes part in SG, and the remaining  $1 - p$  participates in PDG. In the process of game, each individual has two strategies: cooperation and defection. Mutual cooperation yields the reward  $R$ , mutual defection leads to the punishment  $P$ , and the mixed choice gives the cooperator the sucker's payoff  $S$  and the defector the temptation  $T$ . The payoff ranking in SG satisfies:  $T > R > S > P$ . According to the condition of repeated game, it also needs to satisfy:  $2R > T + S$ . Correspondingly, the relations in PDG satisfy:  $T > R > P > S$  and  $2R > T + S$ . To simplify and without losing generality, this paper sets  $R = 1$ ,  $P = 0$ ,  $T = b$  and uses either a positive or a negative value of  $S$  to distinguish game type.  $S = +\delta$  represents SG and  $S = -\delta$  represents PDG. The payoff matrices can be described as [42]

$$M_{SG} = \begin{pmatrix} 1 + \delta & \\ b & 0 \end{pmatrix}, \quad M_{PDG} = \begin{pmatrix} 1 - \delta & \\ b & 0 \end{pmatrix}. \quad (1)$$

Obviously, the parameter  $b$  satisfies:  $1 \leq b \leq 2$ , and the parameter  $\delta$  satisfies:  $0 \leq \delta \leq 1$ . In particular, when  $\delta = 0$ , two payoff matrices are the same, that is, the widely studied weak PDG.

### 2.2 Myopic update rule

The randomly chosen player  $x$  updates his strategy using myopic rule. First, player  $x$  adopts the current strategy according to his own game type to play game with his four nearest neighbors and obtains the actual total payoff  $P_x$ . It is expressed as

$$P_x = \sum_{y \in N_x} P_{xy}, \quad (2)$$

where  $y$  is an arbitrary nearest neighbor of  $x$ , and  $N_x$  is the set of nearest neighbors.  $P_{xy}$  represents the actual payoff of  $x$  by playing game with  $y$ .

Then,  $x$  adopts its anti-strategy of the current strategy (the anti-strategy of cooperation is defection, and the anti-strategy of defection is cooperation) to play a virtual game with its nearest neighbor and obtains the virtual total payoff

$$P_{\bar{x}} = \sum_{y \in N_x} P_{\bar{x}y}, \quad (3)$$

where  $P_{\bar{x}y}$  represents the virtual payoff of  $x$  by playing game with  $y$ .

Finally,  $x$  compares the actual total payoff  $P_x$  with the virtual total payoff  $P_{\bar{x}}$  and determines whether to change the current strategy according to  $W_{x \rightarrow \bar{x}}$ . Its expression is

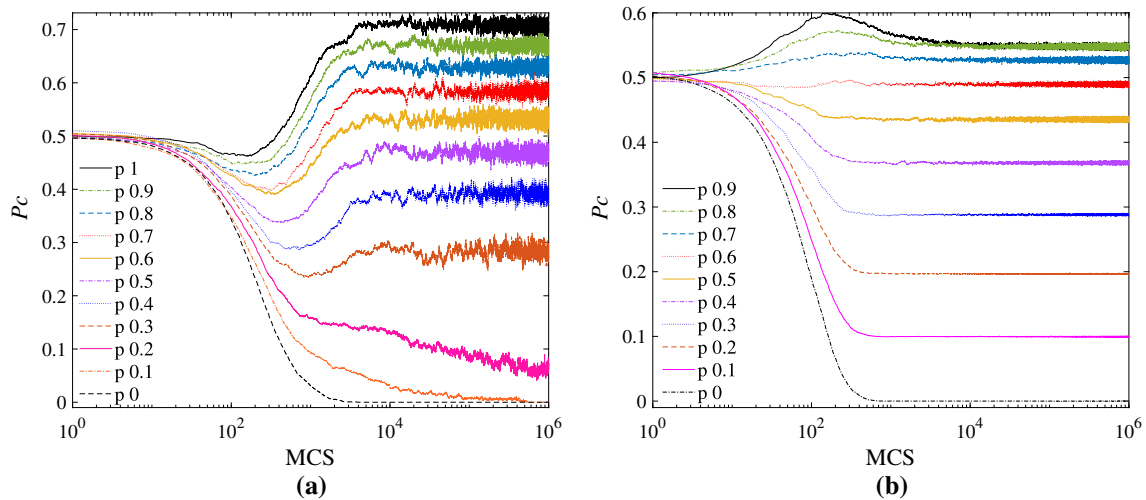


**Fig. 1** The frequency of cooperators  $P_c$  as a function of MCS for the different game parameter  $p$ , where  $k = 0.1$ ,  $b = 1.1$  and  $\delta = 0.3$ , **a** learning rule, **b** self-questioning rule

$$W_{x \rightarrow \bar{x}} = \frac{1}{1 + \exp((P_x - P_{\bar{x}})/k)}, \tag{4}$$

where  $k$  is noise intensity that is used for describing the degree of irrational selection [48–50]. The  $k$  is greater, the individuals are easier to be effected by external environmental noise.

### 2.3 Monte Carlo simulations

Monte Carlo simulations method is also known as statistical sampling method. Its basic concept is to estimate the frequency of something happening through numerous experiments. According to the law of large numbers, the more experiments are conducted, the more accurate the results will be. In one time step, a random player  $x$  is selected and revise its strategy according to myopic update rule. One Monte Carlo step (MCS) is defined as  $N = L \times L$  time steps (that is, each individual has one chance to update his strategy on average). Figure 1 shows the curves of the frequency of cooperators  $P_c$  over time for different  $p$  at  $k = 0.1$ ,  $b = 1.1$  and  $\delta = 0.3$ . Obviously,  $P_c$  tends to stability after  $1 \times 10^4$  MCS for learning mechanism, and  $1 \times 10^3$  MCS for myopic mechanism. The fluctuation for learning mechanism is larger than that for myopic mechanism. To obtain reliable results, time average is required. For learning mechanism, we discarded the first  $2 \times 10^4$  MCS and took the next  $2 \times 10^3$  MCS to calculate the averages. For myopic mechanism, we discarded the initial  $5 \times 10^3$  MCS and took the subsequent  $2 \times 10^3$  MCS to calculate the averages. To reduce the effects of initial states (randomized game type and strategy type) on the results, the final results are average over 20 independent realizations with different initial configurations. All Monte Carlo simulation results in this paper are carried out on the  $100 \times 100$  two-dimensional square lattice.

## 3 Results and discussions

### 3.1 The conversion relationship between evolutionary game model and Ising model

When the game model evolves according to the myopic update rule, there exists the corresponding Ising model [35]. Placing the corresponding game matrices Eq.1 into Eq. 16 of Ref. [35], we can obtain the effective Hamiltonian of PDG and SG respectively, and then analyze the stationary state of the game at  $k = 0$ .

The strength of interaction  $J$  and the external field  $h$  of PDG on two-dimensional square lattice are

$$J = -\frac{1}{4(b - 1 - \delta)}, \tag{5}$$

$$h = -(b - 1 + \delta). \tag{6}$$

The stationary state of the game model can be divided by equation  $J = 0$ ,  $h = 0$  and  $h = \pm 4J$ . In the parameter region of  $0 < \delta < 1$  and  $1 < b < 2$ , the PDG is in the state of complete defection. When  $k = 0$ , the frequency of cooperators  $P_c$  is 0.  $\delta = 0$  is the dividing line between the state of complete defection and the coexisting state of cooperation and defection. When  $k = 0$ , the frequency of cooperators  $P_c$  on the dividing line is less than 0.5.

The strength of interaction  $J$  and external field  $h$  of SG on two-dimensional square lattice are:

$$J = -\frac{1}{4(b - 1 + \delta)}, \tag{7}$$

$$h = -(b - 1 - \delta). \tag{8}$$

In the parameter region of  $0 < \delta < 1$  and  $1 < b < 2$ , the SG is in the coexisting state of cooperation and defection. Thus, the frequency of cooperators  $P_c$  is equal to 0.5 at  $k = 0$ .  $b - 1 - \delta = 0$  is the dividing line

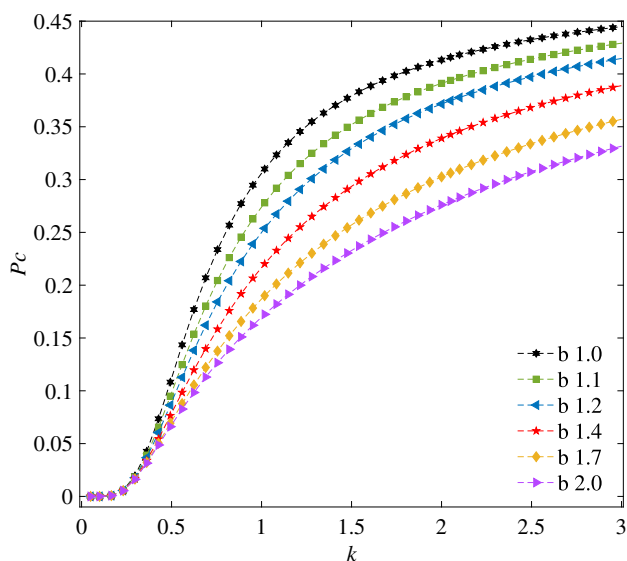


**Fig. 2** The frequency of cooperators  $P_c$  as a function of  $k$  for different game parameter  $b$ , where  $p = 0.0$ ,  $\delta = 0.3$

of the external field, where  $b - 1 - \delta > 0$  is the negative external field and  $b - 1 - \delta < 0$  is the positive external field.  $\delta = 0$  is the dividing line between the state of complete defection and the coexisting state of cooperation and defection. The frequency of cooperators  $P_c$  on this dividing line is less than 0.5 at  $k = 0$ .  $b = 1$  is the dividing line between the state of complete cooperation and the coexisting state of cooperation and defection. The frequency of cooperators  $P_c$  on this dividing line is higher than 0.5 at  $k = 0$ .

### 3.2 The effect of noise parameter $k$ on the frequency of cooperators $P_c$

Section 3.1 describes the ground state of PDG and SG. This section further studies the effect of nonzero noise parameter  $k$  on the frequency of cooperators  $P_c$  at  $p = 0$  and  $p = 1$ , respectively.

When  $p = 0$ , the multi-games model degenerates into spatial PDG. Figure 2 shows the frequency of cooperators  $P_c$  as a function of  $k$  for different  $b$  and fixed  $p = 0$ ,  $\delta = 0.3$ . As is analyzed in Sect. 3.1, when  $k = 0$ , the region is completely defection. When the value of  $\delta$  is fixed, increasing the parameter  $b$  is equal to increasing the negative external field. Thus the frequency of cooperators  $P_c$  will decrease continuously with the increase of  $b$ . As noise parameter  $k$  increased, the frequency of cooperators gradually increases from zero to 0.5 (corresponding to the random selection state). In addition, when  $k$  is fixed, with the increase of  $b$  (corresponding to increasing the temptation of defection), the frequency of cooperators decreases gradually. That is, increasing the gap between  $\delta$  and  $b$  will inhibit the emergence of cooperation.

When  $p = 1$ , the multi-games model degenerates into spatial SG. Figure 3 shows the frequency of cooperators  $P_c$  as a function of  $k$  for different values of the game

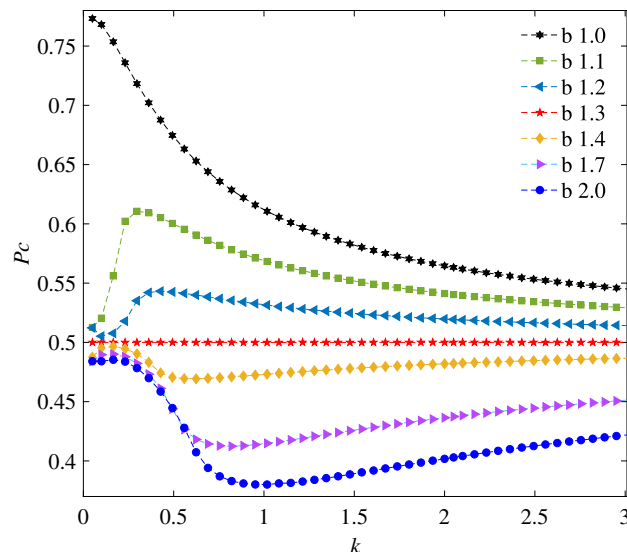


**Fig. 3** The frequency of cooperators  $P_c$  as a function of  $k$  for different game parameter  $b$ , where  $p = 1.0$ ,  $\delta = 0.3$

parameter  $b$  and fixed  $p = 1$ ,  $\delta = 0.3$ . Obviously, when noise intensity is small, the frequency of cooperators  $P_c$  is greater than 0.5 at  $b = 1$ .  $P_c$  is nearly 0.5 when  $b > 1$ . As is known in Sect. 3.1,  $b = 1.3$  is the diving line of the external field. When  $1 < b < 1.3$  (the coexisting state of cooperation and defection under the effect of positive external field), with the increase of noise intensity  $k$ , the frequency of cooperators  $P_c$  first increases and then decreases. When  $1.3 < b \leq 2$  (the coexisting state of cooperation and defection with a negative external field), with the gradual increase of noise intensity  $k$ , the frequency of cooperators  $P_c$  first decreases and then increases. When the value of  $k$  is large enough, no matter what value of  $b$ , the frequency of cooperators is close to 0.5. That is, when  $k$  is large enough, individuals randomly select their own strategies.

### 3.3 The effects of mixing ratio $p$ on the frequency of cooperators

In the multi-games model,  $p$  determines the proportion of players who take part in PDG and SG. The fraction  $p$  of the total players takes part in SG, and the remaining  $1 - p$  participates in PDG. This section discusses the effect of parameter  $p$  on cooperative evolution. Specifically, all individuals take part in the PDG when  $p = 0$ , and all individuals take part in the SG when  $p = 1$ . In other words, with the increase of  $p$  value, the number of players who participate in the SG gradually increases, and the number of players who participates in the PDG gradually decreases.

Figure 4 shows the frequency of cooperators  $P_c$  as a function of  $b$  for different values of  $p$ , fixed the value of  $\delta = 0.3$ ,  $k = 0.1$ . Obviously, for the same value of  $b$ , with the increase of  $p$ , the frequency of cooperators increases gradually. Interestingly, when  $b$  is small, the two curves of  $p = 0.8$  and  $p = 0.9$  are staggered. Thus,

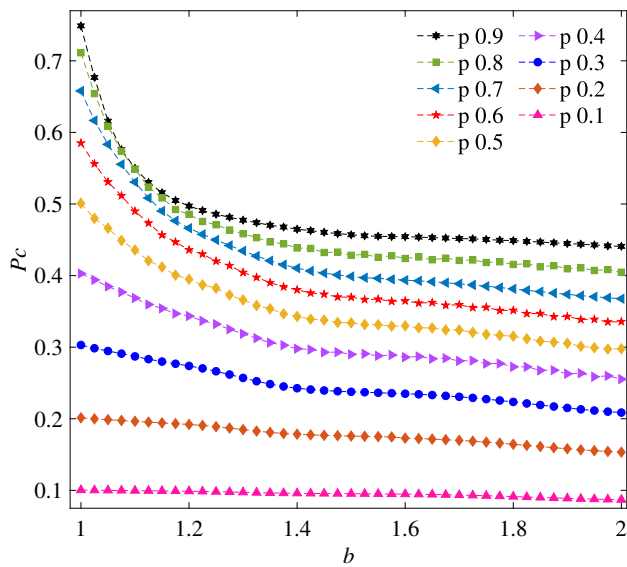


**Fig. 4** The frequency of cooperators  $P_c$  as a function of  $b$  for different mixing ratio  $p$ , where  $\delta = 0.3$  and  $k = 0.1$

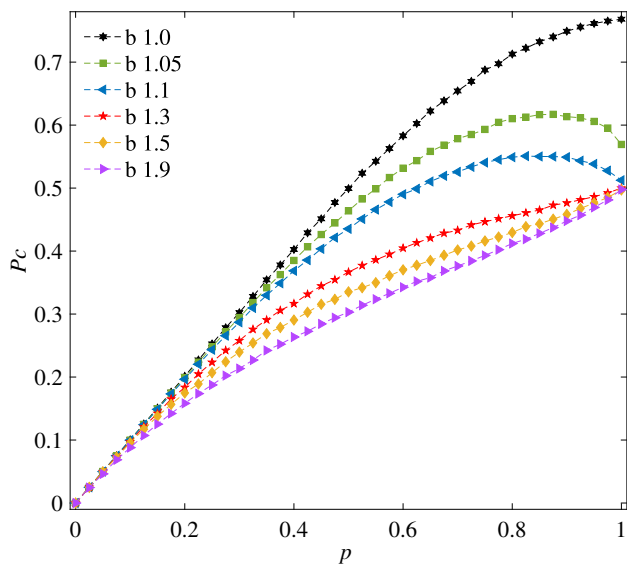


**Fig. 5** The frequency of cooperators  $P_c$  as a function of mixing ratio  $p$  for different game parameter  $b$ , where  $\delta = 0.3$  and  $k = 0.1$

the effect of  $p$  on the frequency of cooperators will be further discussed later when the value of  $b$  is small.

In Fig. 5, the frequency of cooperators  $P_c$  as a function of  $p$  for several  $b$  is shown at  $\delta = 0.3$  and  $k = 0.1$ . The results show that when  $b$  is small, the curves are nonmonotonic. In other words, the mixing of different game types is not simply linear superposition, but that is a process accompanied by emergence and inhibition of cooperation. This phenomenon is similar to the mixing of the ferromagnetic and anti-ferromagnetic in the Ising model randomly. The frustration possibly appeared, and the system may be accompanied by spin glass phase.

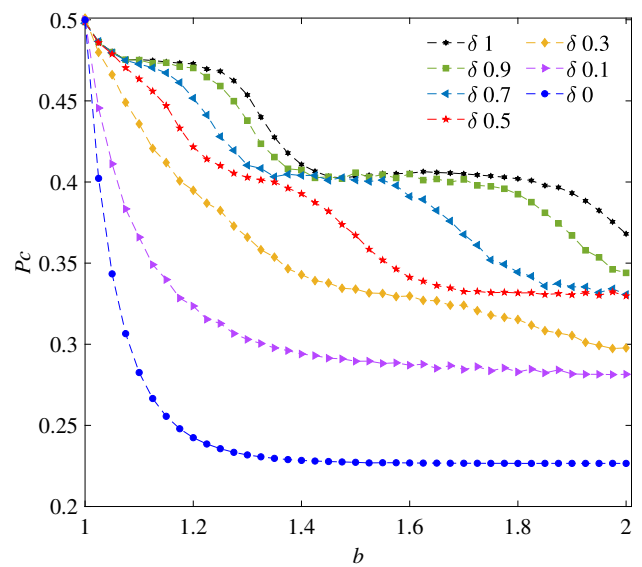


**Fig. 6** The frequency of cooperators  $P_c$  as a function of  $b$  for different game parameter  $\delta$ , where  $p = 0.5$  and  $k = 0.1$

In Fig. 6, the frequency of cooperators  $P_c$  as a function of  $b$  for different values of  $\delta$  at  $p = 0.5$  and  $k = 0.1$ . The results show that  $P_c$  decreases with the increase of  $b$ .  $P_c$  increases with the increase of  $\delta$  for the same value of  $b$ . Specifically, when  $\delta = 0$ , there still exists the cooperators near  $k = 0$ . The reason is that  $\delta = 0$  is the diving line between the state of complete defection and the coexisting state of cooperation and defection. In conclusion, the increase of parameter  $\delta$  promotes the generation of cooperation, while the increase of parameter  $b$  inhibits the generation of cooperation. The final results are determined through the interaction of  $\delta$  and  $b$ , and those curves are nonlinear.

In Fig. 7, the heat maps of the frequency of cooperators for different parameter combinations are shown. Figure 7a shows the frequency of cooperators  $P_c$  gradually increases with the increase of  $\delta$ .  $P_c$  first increases and then decreases with the increase of  $p$ , when  $b = 1.1$  and  $k = 0.1$ . In Fig. 7b, the frequency of cooperators decreases with the increase of  $b$  at  $p = 0.5$  and  $k = 0.1$ . In Fig. 7c, the frequency of cooperators is large only when  $b$  is small fixed  $\delta = 0.3$  and  $k = 0.1$ .

### 3.4 Comparison of learning mechanism and myopic mechanism in multi-games model

In Fig. 8a, the frequency of cooperators  $P_c$  as a function of  $b$  for learning mechanism and myopic mechanism at  $\delta = 0.3$  and  $p = 0.5$  are shown. Obviously, the frequency of cooperators  $P_c$  decreases with the increase of  $b$ . Compared with learning update rule, myopic update rule can still maintain cooperation when  $b$  is large. In Fig. 8b, the frequency of cooperators  $P_c$  as a function of  $\delta$  for learning mechanism and myopic mechanism at  $b = 1.1$  and  $p = 0.5$  are shown. Obviously, the frequency of cooperators  $P_c$  increases with the increase of  $\delta$ . In other words, the larger value of  $\delta$ , the easier emergence

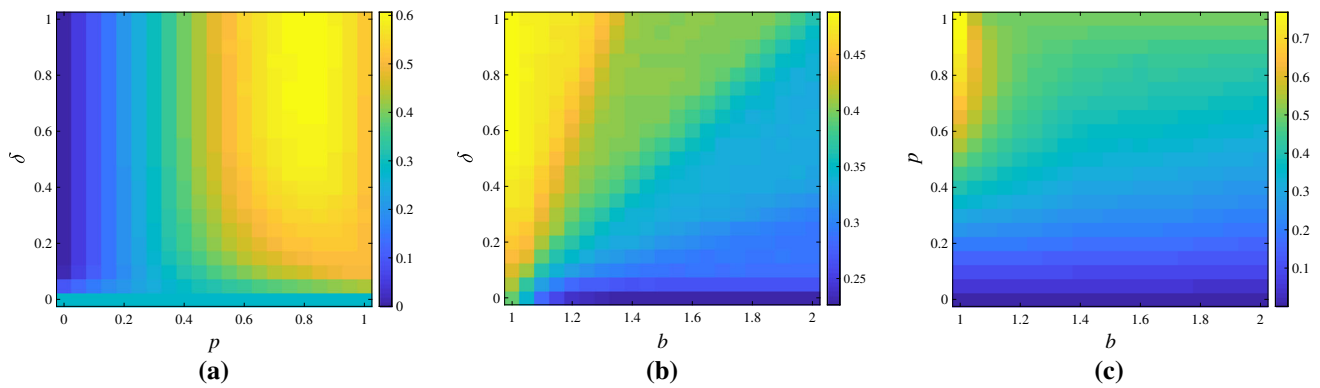


**Fig. 7** The heat maps of the frequency of cooperators  $P_c$  for different parameter combinations: **a**  $b = 1.1, k = 0.1$ ; **b**  $p = 0.5, k = 0.1$ ; **c**  $\delta = 0.3, k = 0.1$

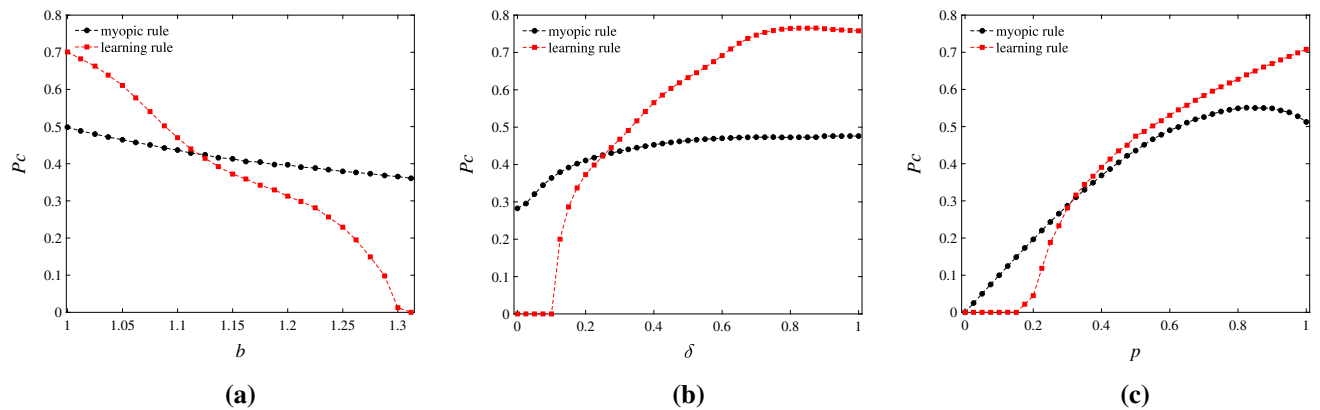


**Fig. 8** The difference between learning rule and myopic rule. **a**  $\delta = 0.3, p = 0.5$ ; **b**  $b = 1.1, p = 0.5$ ; **c**  $\delta = 0.3, b = 1.1$

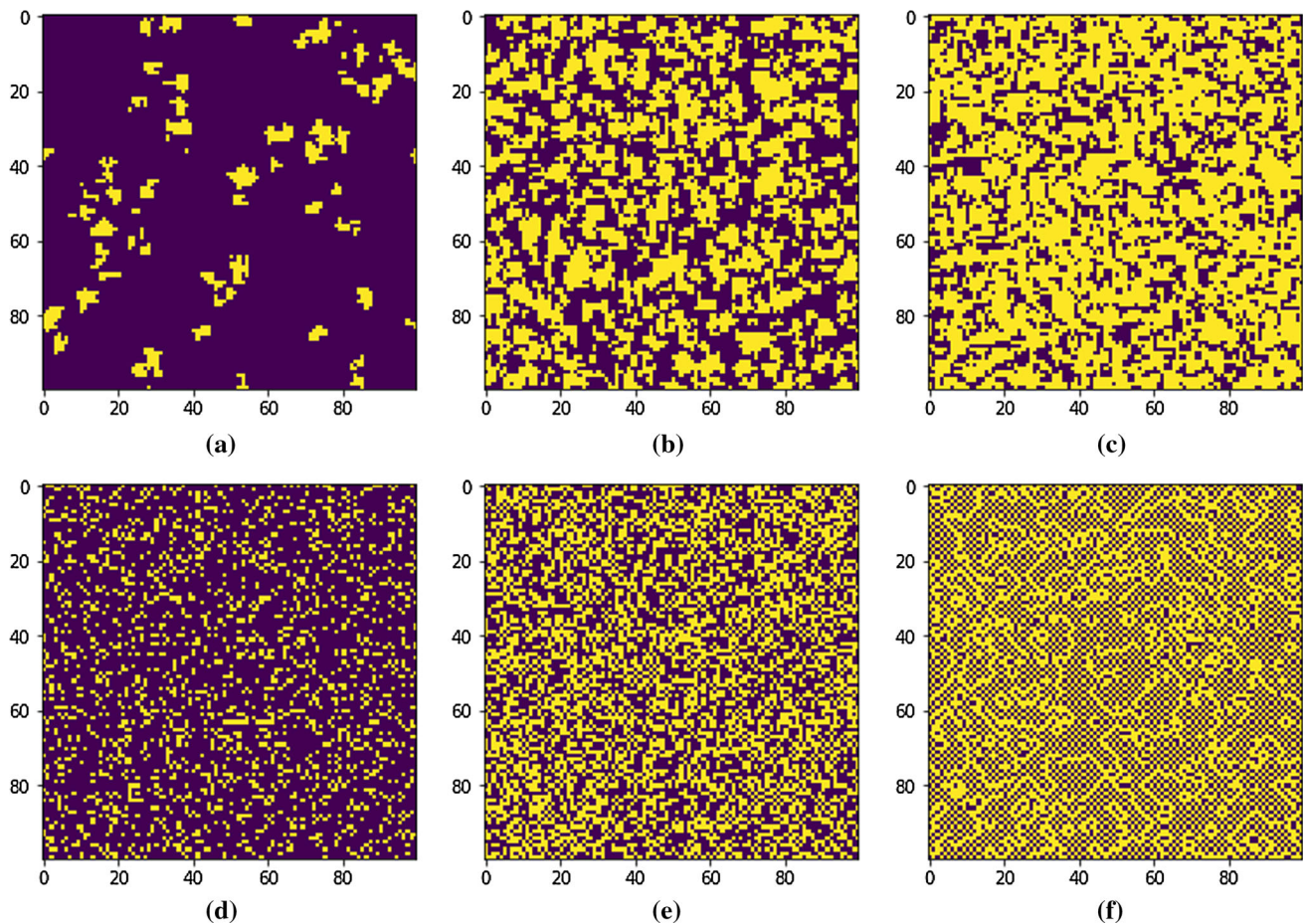
of cooperation. Compared with learning update rule, myopic update rule has weaker effect on the frequency of cooperators  $P_c$ . In Fig. 8c, the frequency of cooperators  $P_c$  as a function of  $p$  for learning mechanism and myopic mechanism at  $\delta = 0.3$  and  $b = 1.1$  are shown. It indicates the frequency of cooperators  $P_c$  increases with the increase of  $p$  for learning mechanism. When  $p$  is small, the cooperators can still exist for myopic mechanism, and the curve does not increase monotonously when  $p$  increases. In other words, mixing ratio  $p$  does not always promote cooperation. To explain the micro differences between learning and myopic mechanism, the snapshots will be used to reveal this phenomenon in the next.

Figure 9 shows the snapshots (spatial distributions of cooperators and defectors) of learning mechanism and myopic mechanism for different values of  $b$  at  $\delta = 0.3$  and  $p = 0.5$ , where yellow and purple represent cooperator and defector respectively. Figure 9a, d is the snapshots for learning mechanism and myopic mechanism at  $p = 0.2$ . Obviously, the cooperators under learning update rule tend to form clusters to resist the invasion of defectors, while the cooperators under myopic update rule tend to form staggered sequences with defectors to increase payoff. Figure 9b, e is the snapshots under learning mechanism and myopic mechanism at  $p = 0.5$ .

Obviously, with the increase of game parameter  $p$ , the clusters formed by the cooperators gradually become larger. However, the spatial configurations formed by the two mechanisms are significantly different. Figure 9c, f is the snapshots under learning mechanism and myopic mechanism at  $p = 0.9$ . Obviously, cooperators form larger clusters under learning mechanism, and cooperators and defectors occur alternately under myopic mechanism. Cooperators or defectors have no obvious tendency to form clusters, and most of the cooperators or defectors are isolated. This spatial configuration is quite similar to anti-ferromagnetic Ising model under frustration. Specifically, this so-called role-separating patterns is a checkerboard-like distribution of cooperators and defectors on square lattice have been observed in Ref. [51–53]. In short, there are significant differences in the stationary space configurations formed by the time evolution of learning mechanism and myopic mechanism.

### 4 Conclusion

In this paper, we use Monte Carlo simulation method to study a spatial evolutionary multi-games model under myopic update rule. Initially, the players select PDG



**Fig. 9** Spatial distributions of cooperators [yellow (light gray)] and defectors [purple (dark gray)] for different the mixing ratio  $p$  and fixed  $\delta = 0.3$ ,  $b = 1.1$ . The snapshots under learning mechanism are shown in panels **a–c**, and the value of  $p$  is in sequence of 0.2, 0.5, and 0.9. The snapshots under myopic mechanism are shown in panels **d–f**, and the value of  $p$  is in sequence of 0.2, 0.5, and 0.9

or SG randomly according to the mixing ratio  $p$ . Then, individuals update their strategies using myopic rule. The main results are as follows: (1) the initial state of PDG and SG are obtained by the relationship between spatial evolutionary game model and Ising model when the noise parameter  $k$  is zero. In the parameter region of  $0 < \delta < 1$  and  $1 < b < 2$ , PDG is in the state of complete defection, and SG is in the coexisting state of cooperation and defection; (2) the effect of noise parameter  $k$  on the frequency of cooperators  $P_c$  varies with the parameter spaces. In the state of complete defection, the frequency of cooperators increases with the increase of  $k$  and gradually approaches 0.5. In the state of the coexisting state of cooperation and defection under the positive external field, the frequency of cooperators first increases and then decreases with the increase of  $k$  and finally approaches 0.5; (3) the effect of the mixing ratio  $p$  on the frequency of cooperators is nonmonotonic. When the value of  $b$  is small, the frequency of cooperators first increases and then decreases; (4) the effects of the game parameters  $\delta$  and  $b$  on the frequency of cooperators are mutually related and restricted. When  $b$  is fixed, the frequency of cooperators increases with

the increase of  $\delta$ , and when  $\delta$  is fixed, the frequency of cooperators decreases with the increase of  $b$ . In particular, when  $\delta = 0$ , the game model degenerates into weak PDG; (5) by comparing the learning mechanism and myopic mechanism in the multi-games model, the cooperators under learning update rule tend to form clusters to resist the invasion of defectors, while the cooperators under myopic update rule tend to form a staggered relationship with the defectors to increase individual payoff.

**Acknowledgments** The authors would like to thank Doctor Jinhai Li for his valuable comments and suggestions on the preliminary draft. This work was supported by the National Natural Science Foundation of China (Grant No. 11947041).

## Author contributions

All the authors contributed equally to this study.

**Data Availability Statement** This manuscript has no associated data or the data will not be deposited. [Authors’

comment : Since our simulation results are based on the average of multiple random initial results, different number of replications and model evolution steps may cause slight differences in the test results. Therefore, we did not save the experimental data.]

## References

1. A. Nowak, M. May, *Nature* **359**, 826–829 (1992)
2. G. Szabó, C. Tóke, *Phys. Rev. E* **58**, 69–73 (1998)
3. G. Szabó, G. Fáth, *Phys. Rep.* **446**, 97–216 (2007)
4. C. Hauert, M. Doebeli, *Nature* **428**, 643–646 (2004)
5. C. Hauert, G. Szabó, *Am. J. Phys.* **73**, 405–414 (2005)
6. F.C. Santos, J.F. Rodrigues, J.M. Pacheco, *Phys. Rev. E* **72**, 056128 (2005)
7. F.C. Santos, J.M. Pacheco, *Phys. Rev. Lett.* **95**, 098104 (2005)
8. F.C. Santos, J.F. Rodrigues, J.M. Pacheco, *Proc. R. Soc. B* **273**, 51–55 (2006)
9. Z. Wang, L. Wang, A. Szolnoki, M. Perc, *Eur. Phys. J. B* **88**, 124 (2015)
10. Y. Wu, S.H. Zhang, Z.P. Zhang, *Sci. Rep.* **8**, 15616 (2018)
11. C.B. Sun, C. Luo, *Appl. Math. Comput.* **374**, 125063 (2020)
12. A. Szolnoki, G. Szabó, M. Perc, *Phys. Rev. E* **83**, 036101 (2011)
13. Z. Wang, C.Y. Xia, S. Meloni, C.S. Zhou, Y. Moreno, *Sci. Rep.* **3**, 3055 (2013)
14. Y.N. Geng, C. Shen, K.P. Hu, L. Shi, *Physica A* **503**, 540–545 (2018)
15. Q. Song, Z.H. Cao, R. Tao, W. Jiang, C. Liu, J.Z. Liu, *Appl. Math. Comput.* **368**, 124798 (2020)
16. F. Fu, C. Hauert, M.A. Nowak, L. Wang, *Phys. Rev. E* **78**, 026117 (2008)
17. X.P. Li, S.W. Sun, C.Y. Xia, *Appl. Math. Comput.* **361**, 810–820 (2019)
18. W.X. Wang, J. Ren, G.R. Chen, B.H. Wang, *Phys. Rev. E* **74**, 056113 (2006)
19. F. Shu, Y.J. Liu, X.W. Liu, X.B. Zhou, *Appl. Math. Comput.* **346**, 480–490 (2019)
20. M. Perc, A. Szolnoki, *Phys. Rev. E* **77**, 011904 (2008)
21. M. Perc, A. Szolnoki, *BioSystems* **99**, 109–125 (2010)
22. A. Szolnoki, M. Perc, *EPL* **110**, 38003 (2015)
23. I.S. Lim, P. Wittek, *Phys. Rev. E* **98**, 062113 (2018)
24. C. Shen, C. Chu, L. Shi, M. Perc, Z. Wang, *R. Soc. Open. Sci.* **5**, 180199 (2019)
25. X.J. Wang, C.L. Gu, J.H. Zhao, J. Quan, *Phys. Rev. E* **100**, 022411 (2019)
26. L.M. Zhang, C.W. Huang, H.H. Li, Q.N. Dai, *EPL* **126**, 18001 (2019)
27. M.R. Arefin, J. Tanimoto, *Phys. Rev. E* **102**, 032120 (2020)
28. A. Matsui, *J. Econ. Theory* **57**, 343–362 (1992)
29. G. Szabó, A. Szolnoki, *J. Theor. Biol.* **299**, 81–87 (2012)
30. Z. Danku, Z. Wang, A. Szolnoki, *EPL* **121**, 18002 (2018)
31. J. Shi, J.Z. Liu, M. Perc, Z.H. Deng, Z. Wang, *Chaos* **31**, 123113 (2021)
32. T. Qiu, T. Hadzibeganovic, G. Chen, L.X. Zhong, X.R. Wu, *Comput. Phys. Commun.* **181**, 2057–2062 (2010)
33. K. Gao, W.X. Wang, B.H. Wang, *Physica A* **380**, 528–538 (2007)
34. Q. Miao, J. Wang, M.L. Hu, F. Zhang, Q.S. Zhang, C.Y. Xia, *Eur. Phys. J. Plus* **129**, 8 (2014)
35. B. Yang, X.T. Li, W. Chen, J. Liu, X.S. Chen, *Commun. Theor. Phys.* **66**, 439–446 (2016)
36. B. Yang, M. Fan, W.Q. Liu, X.S. Chen, *Acta. Phys. Sin.* **66**, 196401 (2017)
37. B. Yang, Y.W. Zhang, W.Q. Liu, X.S. Chen, *Sci. China Phys. Mech. Astron.* **48**, 050501 (2018)
38. B. Yang, J.H. Li, *Int. J. Mach. Learn. Cybern.* **12**, 2317–2325 (2021)
39. K. Hashimoto, *J. Theor. Biol.* **241**, 669–675 (2006)
40. K. Hashimoto, *J. Theor. Biol.* **345**, 70–77 (2014)
41. A. Szolnoki, M. Perc, *EPL* **108**, 28004 (2014)
42. Z. Wang, A. Szolnoki, M. Perc, *Phys. Rev. E* **90**, 032813 (2014)
43. J.H. Qin, Y.M. Chen, Y. Kang, M. Perc, *EPL* **118**, 18002 (2017)
44. Z.B. Li, D.Y. Jia, H. Guo, Y.N. Geng, C. Shen, Z. Wang, X.L. Li, *Appl. Math. Comput.* **351**, 162–167 (2019)
45. X.P. Li, H.B. Wang, G. Hao, C.Y. Xia, *Phys. Lett. A* **384**, 126414 (2020)
46. X.P. Li, G. Hao, H.B. Wang, C.Y. Xia, M. Perc, *J. Stat. Mech.* **1**, 013403 (2020)
47. C.W. Liu, J. Wang, X.P. Li, C.Y. Xia, *Phys. Lett. A* **384**, 126928 (2020)
48. G. Szabó, J. Vukov, A. Szolnoki, *Phys. Rev. E* **72**, 047107 (2005)
49. J. Vukov, G. Szabó, A. Szolnoki, *Phys. Rev. E* **73**, 067103 (2006)
50. A. Szolnoki, J. Vukov, G. Szabó, *Phys. Rev. E* **80**, 056112 (2009)
51. G. Szabó, A. Szolnoki, M. Varga, L. Hanusovszky, *Phys. Rev. E* **82**, 026110 (2010)
52. A. Szolnoki, M. Perc, *Phys. Rev. E* **89**, 022804 (2014)
53. M.A. Amaral, M. Perc, L. Wardil, A. Szolnoki, E.J. da Silva Júnior, J.K.L. da Silva, *Phys. Rev. E* **95**, 032307 (2017)